Journal of Marine Science and Technology, Vol. 25, No. 6, pp. 775-783 (2017)
DOI: 10.6119/JMST-017-1226-19

DYNAMIC RESPONSE ANALYSIS OF MICRO-GRID WITH OCEAN THERMAL ENERGY CONVERSION

Chia-Yu Hsu, Ming-Wang Chen, and Pei-Hwa Huang

Key words: Ocean Thermal Energy Conversion (OTEC), micro-grid, distributed generation, wind generation, renewable energy.

ABSTRACT

The main purpose of this paper is to analyze the dynamic responses of micro-grid with Ocean Thermal Energy Conversion (OTEC) system. The power sources of the studied micro-grid system include an OTEC generator and a wind generator. Three different types of OTEC generation systems, i.e., open-cycle, closed-cycle, and hybrid-cycle, are considered, under the conditions with the same temperature of sea water and output of generator. When the system operates in an islanding or grid-connected mode, the responses subject to load variation are quite different. As the system operates in the grid-connected mode, the voltage and frequency are less affected by the load changes; while the system operates under the islanding mode, affected voltage and frequency can be regulated by the exciter and the governor respectively and will return to a new stable state. According to the results, it is shown that the OTEC system can be regarded as a steady and reliable power supply in the micro-grid.

I. INTRODUCTION

The demand for environmental protection and the progressive exhaustion of traditional fossil energy sources have increased the interest in integrating renewable energy sources into the existing power systems. Renewable energy plays a key role in reducing greenhouse gases which have resulted in global warming. The power systems with renewable energy resources near power loads are utilized to provide the electrical energy to the consumers. The power systems with renewable energy resources can operate in off-grid and grid connected modes (Kundur, 1994; Anderson, 2002).

Paper submitted 05/04/16; revised 12/05/17; accepted 12/13/17. Author for correspondence: Pei-Hwa Huang (e-mail: B0104@mail.ntou.edu.tw).
Department of Electrical Engineering, National Taiwan Ocean University, Keelung, Taiwan, R.O.C.

The ocean thermal energy concept was proposed as early as 1881 by French physicist Jacques d'Arsonoval. The sun continuously heats the ocean, maintaining the temperatures of water at surface significantly higher than that of the deep ocean (Vijayakrishna Rapaka et al., 2013). Ocean thermal energy conversion (OTEC) is a renewable energy technology that makes use of the temperature difference between the surface and the depth of the ocean to produce the electricity by running a low-pressure turbine (Vega, 1995; Vega, 2002)

Yeh et al. (2014) proposed that a larger maximum net output can be obtained by employing a higher temperature of the warm seawater. Najafi et al. (2011) proposed that a multi-objective optimization via genetic algorithm provides a set of optimal solutions to minimize the total pumping power and heat transfer area as objectives. Goto et al. (2012) presented a simulation model of the evaporator and separator in an OTEC plant using the Uehara cycle that is constructed by using some physical laws and experimental data. Shakil et al. (2013) proposed that the site of Bangladesh is naturally gifted area to establish OTEC as Bangladesh lies just beneath the Tropic of Cancer and on the shore of the Bay of Bengal, the two vital elements: constant sunlight and large littoral areas needed for OTEC can easily be found in this region. Urayoshi et al. (2014) presented that the evaporator is one of the most important devices for OTEC plants. Matsuda et al. (2015) designed a PI controller for the liquid level control of separator in an OTEC plant with Uehara cycle by considering some kinds of disturbances Lee et al. (2016) identified the thermal dispersion characteristics of coastal waters to consider their physical properties using a field observation and a three-dimensional numerical modeling with Computational Fluid Dynamics (CFD) Mudaliyar and Mishra (2016) examined the dynamic stability of solar-concentrated OTEC (SC-OTEC) plant in a multi-machine power system scenario.

The main purpose of this paper is to analyze the dynamic responses of a micro-grid with the OTEC system as one of the power sources. The tasks of the study are as follows. Firstly, the model of each individual element is to be developed. Secondly, the established element models are further integrated intoa model for the whole power system. Finally, dynamic analysis is performed on the power system with the OTEC system under off-grid and grid-connected operations.

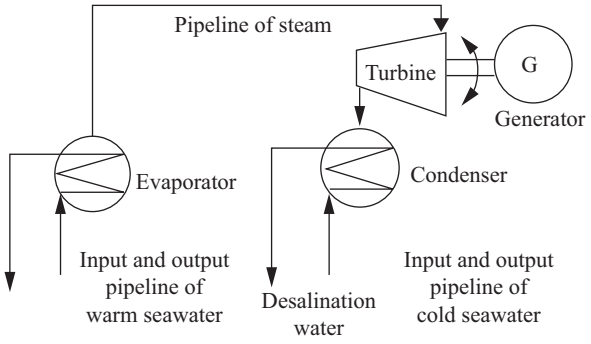

Fig. 1. Model of open-cycle OTEC system (Avery and Wu, 1994).

II. SYSTEM MODEL

The OTEC system is composed of evaporator, condenser, steam turbine, generator, working fluid, and pumps. In this work, three different types of OTEC generation systems, i.e., open-cycle, closed-cycle, and hybrid-cycle are considered (Avery and Wu, 1994; Ghosh, 2011; Kim et al., 2016).

1. Open-Cycle OTEC

The open-cycle OTEC system model is shown in Fig. 1 (Avery and Wu, 1994; Ghosh, 2011; Kim et al., 2016). In an open-cycle OTEC system, the warm seawater is used as the working fluid. The warm seawater is flash evaporated in a vacuum chamber and steam is produced. The steam expands through a low-pressure turbine that is coupled with a generator to produce electricity. The steam leaving the turbine is then condensed by cold deep seawater through a cold water pipe. If a surface condenser is used in the system, the condensed steam remains separated from the cold seawater and provides a supply of desalinated water. However, a further disadvantage of open-cycle operation is the need to provide vacuum pumps to remove fixed gases that are removed from the seawater along with the steam that forms the working fluid to drive the turbine. If allowed to accumulate in the condenser, these fixed gases would rapidly degrade the operation of the condenser. The power needed to operate the vacuum pumps can significantly reduce the net power output (Avery and Wu, 1994).

The output mass flow rate of warm seawater is

$$m_{wso} = m_{wsi} - m_{st} \tag{1}$$

where m_{wsi}, m_{wso} are input and output mass flow rate of warm seawater, m_{st} is mass flow rate of evaporated seawater. All of these units are kg/s.

The heat quantity of warm seawater Q_E (kW) is

$$Q_E = c_p (T_{wsi} m_{wsi} - T_{wso} m_{wso}) \tag{2}$$

where c_p is specific heat of water with normal temperature (4.181 kJ/kg·K), T_{wsi} and T_{wso} are input and output temperature of warm seawater (°C), respectively.

The output pressure of steam turbine is computed by expansion rate

$$P_{tb} = P_{st} / \eta_{\exp} \tag{3}$$

where P_{st} and P_{tb} are input and output pressure of steam turbine (kPa) and $\eta_{\exp}$ is expansion rate of steam turbine, of which the value used in this paper is 1.89.

The different enthalpy of steam turbine (Δh_{tb}) is

$$\Delta h_{tb} = h_{st} - h_{tb,\exp} \tag{4}$$

where h_{st} and $h_{tb,\exp}$ are input and output enthalpy of steam turbine (kJ/kg), respectively.

The generator produces power W_{gen} (kW) is

$$W_{gen} = \eta_{gen} \eta_{shaft} \eta_{tb} m_{st} \Delta h_{tb} \tag{5}$$

where η_{gen}, η_{brn}, and η_{tb} are the efficiency of generator, shaft, and steam turbine, respectively.

The mass flow rate of cold seawater of discharge is

$$m_{cso} = m_{csi} + m_{st} \tag{6}$$

where m_{csi} and m_{cso} are input and output mass flow rate of cold seawater, m_{st} is mass flow rate of evaporated gas (kg/s).

The heat quantity of cold seawater Q_C (kW) is

$$Q_C = c_p (T_{cso} m_{cso} - T_{csi} m_{csi}) \tag{7}$$

where c_p is specific heat of water with normal temperature (4.181 kJ/kg·K), m_{csi} and m_{cso} are input and output mass flow rate of cold seawater, T_{csi} and T_{cso} are input and output temperature of cold seawater (°C), respectively.

2. Closed-Cycle OTEC

The closed-cycle system uses a working fluid, such as ammonia, pumped around a closed loop (Ghosh, 2011; Kim et al., 2016). This design has three components: a pump, turbine and heat exchanger (evaporator and condenser). The temperature range available for the Rankine cycle is restricted to about half the difference in temperature between warm and cold water by the requirements that a temperature difference must exist to enable heat to be transferred from the warm water to the working fluid in the evaporator, and another temperature difference must exist for heat transfer from the working fluid to cold water in the condenser (Avery and Wu, 1994). Warm surface seawater is pumped through a heat exchanger that vaporizes the fluid with a low boiling point. Then the working fluid turns into vapor and runs the turbo generator as shown in Fig. 2 (Avery and Wu, 1994).

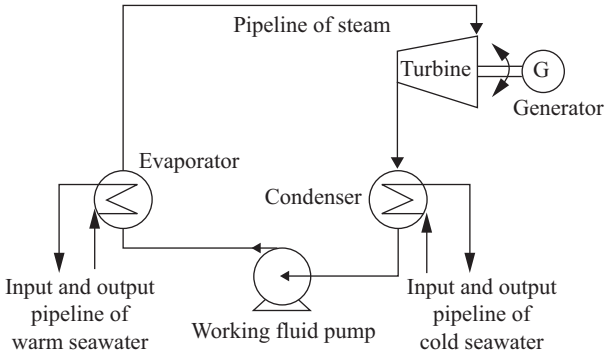

Fig. 2. Model of closed-cycle OTEC system (Avery and Wu, 1994).

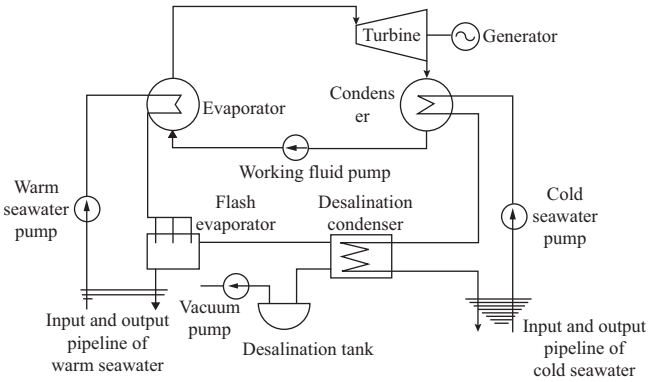

Fig. 3. Model of hybrid-cycle OTEC system (Ghosh, 2011).

Later the steam is condensed through heat exchange with the cold pumped deep sea water causing the liquefaction again. Thus the cycle goes round like this and keeps moving the turbine.

The heat balance equation of evaporator is

$$Q_E = m_{wf}(h_1 - h_4) = m_{wsi} c_p (T_{wsi} - T_{wso}) \tag{8}$$

where Q_E is heat quantity of warm seawater (kW), m_{wf} is mass flow of working fluid, m_{wsi} is input mass flow of warm seawater (kg/s), h_1 and h_4 are input and output enthalpy of working fluid of evaporator (kJ/kg·K), and T_{wsi} and T_{wso} are input and output temperature of warm seawater (°C).

The heat transfer coefficient relates to the effective area of evaporator and the heat balance equation is

$$Q_E = U_E A_E \Delta T_{lm,E} \tag{9}$$

where U_E is heat transfer coefficient (kW/m^2·K), A_E is heat exchange area (m^2), and $\Delta T_{lm,E}$ is logarithmic mean temperature difference (°C). All the above are related with evaporator.

The logarithmic mean temperature difference is

$$\Delta T_{lm,E} = [(T_{wsi} - T_E) - (T_{wso} - T_E)] / \ln \frac{(T_{wsi} - T_E)}{(T_{wso} - T_E)} \tag{10}$$

where T_E is temperature of evaporator, T_{wsi} and T_{wso} are input and output temperature of warm seawater (°C).

The heat balance equation of condenser is

$$Q_C = m_{wf}(h_2 - h_3) = m_{csi} c_p (T_{cso} - T_{csi}) \tag{11}$$

where Q_C is heat quantity of cold seawater (kW), m_{csi} is input mass flow of cold seawater (kg/s), h_2 and h_3 are input and output enthalpy of working fluid of condense side (kJ/kg·K).

The heat transfer coefficient relates to the effective area of condenser, its heat balance equation is equal to

$$Q_C = U_C A_C \Delta T_{lm,C} \tag{12}$$

where U_C is heat transfer coefficient (kW/m^2·K), A_C is heat exchange area (m^2), $\Delta T_{lm,C}$ is logarithmic mean temperature difference (°C). All the above are related with condenser.

The logarithmic mean temperature difference $\Delta T_{lm,C}$ can be computed as

$$\Delta T_{lm,C} = [(T_C - T_{csi}) - (T_C - T_{cso})] / \ln \frac{(T_C - T_{csi})}{(T_C - T_{cso})} \tag{13}$$

where T_C is temperature of condenser, T_{csi} and T_{cso} are input and output temperature of cold seawater (°C).

3. Hybrid-Cycle OTEC

The hybrid-cycle OTEC system is one of the variations of the standard open-cycle OTEC system. It is a blend of both the open and closed cycles designed to produce both electric power and fresh water as the products. The hybrid cycle is an attempt to combine the best features and avoid the worst features of the open and closed cycles. The principal disadvantages of open-cycle system are the low pressure available to operate the turbine as well as the large specific volumes that must be used by the steam turbine. The low cycle efficiency due to the small temperature difference combined with the large specific volumes requires a very large turbine (Avery and Wu, 1994). Hybrid-cycle OTEC system model is shown in Fig. 3 (Ghosh, 2011). In this system, warm seawater enters a vacuum chamber where it is evaporated into steam, which is similar to the open-cycle evaporation process. The steam vaporizes the working fluid of a closed-cycle loop on the other side of a vaporizer. The vaporized fluid then drives a turbine to generate electricity. The steam condenses within the heat exchanger and provides desalinated water.

4. Pumps Model

When a fluid of density ρ and dynamic viscosity η flows with a volumetric flow rate of q_p through a pipe of length L_p

and diameter D_p, its average flow speed is (Kim et al., 2016)

$$u = q_p / A_p \tag{14}$$

where u average flow speed, A_p is cross-sectional area of the cylindrical pipe.

Pumping power of warm or cold seawater may be written as

$$W_p = q_p \Delta P_{loss} / \eta_p \tag{15}$$

where W_p is pumping power of warm or cold seawater, η_p is efficiencies of the pump, and ΔP_{loss} is the pressure loss along the pipe of length (Kim et al., 2016)

$$\Delta P_{loss} = C_D P_{dyn} L_p / D_p \tag{16}$$

$$C_D = [1.8 \log_{10}(\mathrm{Re}) - 1.64]^{-2} \tag{17}$$

$$\mathrm{Re} = (4 q_p) / (\pi v D_p) \tag{18}$$

$$P_{dyn} = 0.5 \rho u^2 \tag{19}$$

where C_D is the drag factor, Re is Reynolds number, and v is the kinematics viscosity of seawater.

5. Governor Model

The turbine of the studied OTEC is characterized by the employed working fluid with low-pressure ratios and relatively high mass flow. Fig. 4 shows the block diagram of the employed governor and turbine model that is the type without steam feedback (Kundur, 1994; Wang and Huang, 2010), in which $\Delta\omega_r$ is speed difference. K is speed droop. ΔP is total speed change rate. P_{tb} is inlet torque of turbine. P_{GV} is inlet vapor of turbine. P_M is inlet torque of generator. T_1, T_2, T_{CH} are time delay. $P_{\max}$, $P_{\min}$ are inlet air limits.

6. Synchronous Machine Model

Synchronous generators serve as the principal source of electric energy in power systems. The equivalent circuit of the model is shown in Fig. 5 and Fig. 6 (Kundur, 1994), where φ_d and φ_q are stator-side flux linkage of d-axis and q-axis, φ'_{fd} is rotor-side excitation winding flux linkage. φ'_{kd}, φ'_{kq1}, and φ'_{kq2} are rotor-side damping flux linkage of d-axis and q-axis. ω_R is rotor speed. i_d and i_q are the stator-side current of d-axis and q-axis. i'_{fd} is rotor-side excitation winding current. i'_{kd}, i'_{kq1}, i'_{kq2} are rotor-side damping current of d-axis and q-axis. R_s is stator-side winding resistance. R'_{fd} is rotor-side excitation winding resistance. R'_{kd}, R'_{kq1}, R'_{kq2} are rotor-side damping winding resistance of d-axis and q-axis.

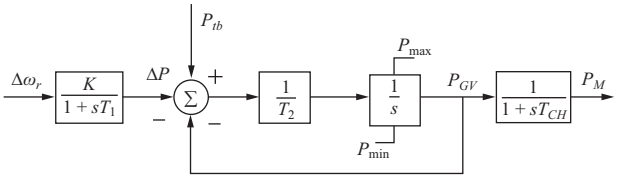

Fig. 4. The block diagram of governor model (Kundur, 1994; Wang and Huang, 2010).

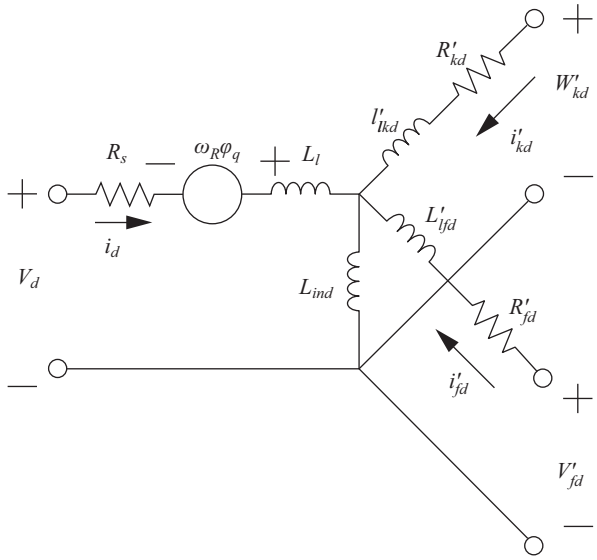

Fig. 5. Equivalent circuit of *d*-axis (Kundur, 1994).

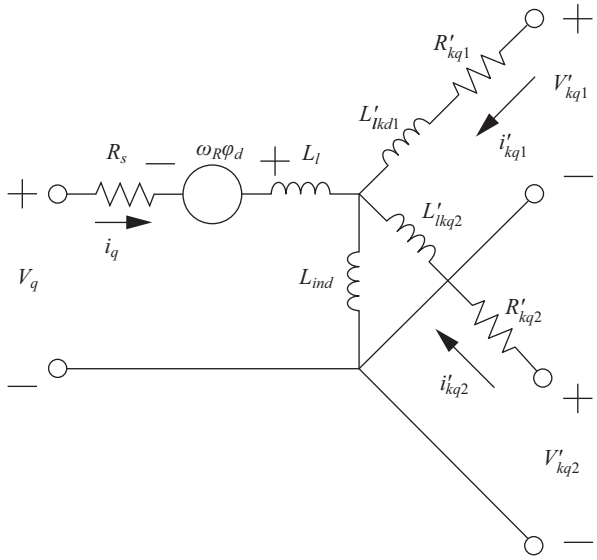

Fig. 6. Equivalent circuit of *q*-axis (Kundur, 1994).

7. Excitation Model

Excitation system control will directly influence the voltage stability. It produces DC voltage for current to flow in the field

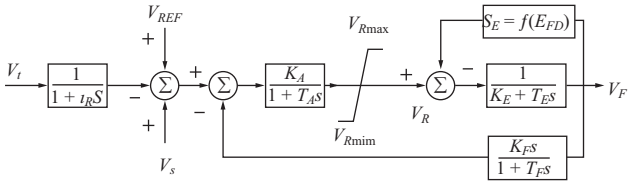

Fig. 7. The block diagram of excitation model (Kundur, 1994).

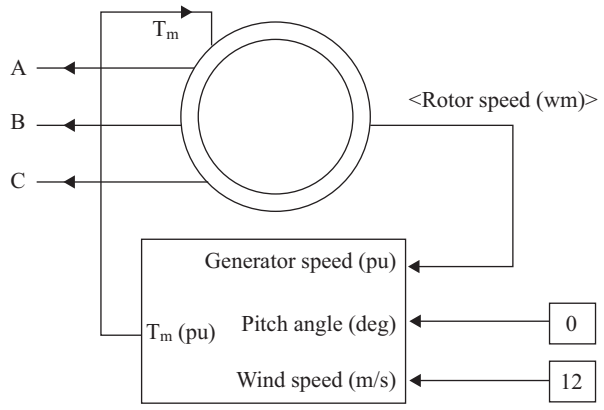

Fig. 8. Model of wind turbine generation system (Ahmad and Siddiqui, 2014).

windings of the generator. There is a direct relationship between the generator terminal voltage and the exciter voltage as shown in Fig. 7 (Kundur, 1994), in which V_t is terminal voltage of generator. V_{REF} is reference value of stator voltage. V_F is the excitation voltage of generator. V_s denotes the extra signal from Power System Stabilizer (PSS). K's and T's are gains and time constants of transfer functions.

8. Wind Generation

The wind turbine model as shown in Fig. 8 is based on the steady-state power characteristics of the turbine. The output power of the turbine is given by the following equation (Ahmad and Siddiqui, 2014).

$$P_m = \tfrac{1}{2} C_\rho(\lambda, \beta) \rho A V^3 \tag{20}$$

$$\lambda = \omega K_b / V \tag{21}$$

where C_p is performance coefficient, λ is tip-speed ratio, β is pitch angle, ρ is air density, V is wind speed, and K_b is a constant.

It was demonstrated that for fixed speed Wind Turbine Generation System (WTGS) the power modeling from curves under the assumption of stationary wind speed is sufficient for the power system studies. The characteristics of wind turbine between turbine speed referred to generator side and powers are shown in Fig. 9 (Ahmad and Siddiqui, 2014).

III. CASE STUDY

1. Study System

This paper aims to analyze the dynamic responses of a micro-

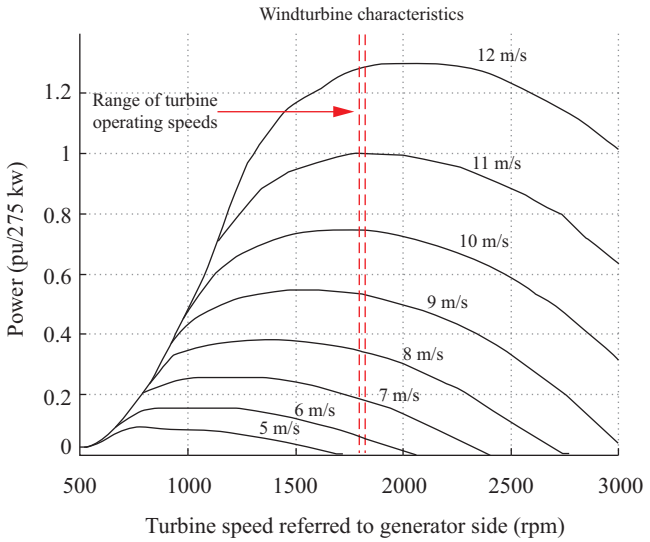

Fig. 9. Typical characteristics of wind turbine (Ahmad and Siddiqui, 2014).

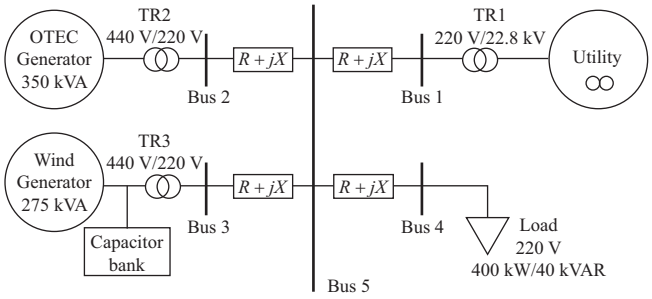

Fig. 10. Single line diagram of the power system.

grid with OTEC generation. A single line diagram of the power system is shown in Fig. 10. The power system under study consists of a utility and two kinds of renewable resources, including OTEC and wind generation.

2. Comparison of OTEC with Different Types

Studies are made to compare the three types of OTEC generation system operation under constant output power. The simulation results are listed in Table 1. The "Temperature" rows denote input and output warm seawater and cold seawater. The "Mass flow" rows concern input and output warm seawater and cold seawater. The "Heat quantity" rows give the absorption and discharge power. And finally the "Pumps power" rows tabulate the power of warm, cold water, and working fluid.

Table 1 shows that open-cycle demands large amount of seawater, its power of water pumps are the most, and its heat quantity is better than that of closed-cycle. Besides, open-cycle has the lowest output temperature of warm seawater and the highest output temperature of cold seawater. The open-cycle uses seawater as working fluid and needs not working fluid pump to pass the seawater for evaporator. The closed-cycle and hybrid-cycle demand less seawater, and the output temperature, mass flow, and pumps are the same. This is because closed-cycle and hybrid-

Table 1. OTEC system analyzes with different types.

		Open-Cycle	Closed-Cycle	Hybrid-Cycle
Temperature	Inlet warm water	26°C	26°C	26°C
	Outlet warm water	22.7°C	23.96°C	23.96°C
	Inlet cold water	5°C	5°C	5°C
	Outlet cold water	9.85°C	7.44°C	7.44°C 7.44°C
Mass flow	Inlet warm water	1115.4 kg/s	952.4 kg/s	952.4 kg/s
	Outlet warm water	1109.1 kg/s	952.4 kg/s	952.4 kg/s
	Inlet cold water	756 kg/s	758.3 kg/s	758.3 kg/s
	Outlet cold water	762.3 kg/s	758.3 kg/s	758.3 kg/s
Heat quantity	Evaporator	16010 kW	8143 kW	16811 kW
	Condoner	15580 kW	7769 kW	16461 kW
Pump	Warm water	21.01 kW	13.4 kW	13.4 kW
	Cold water	6.75 kW	6.8 kW	6.8 kW
	Working fluid	(N/A)	4.3kW 4.3 kW	4.3 kW
	Output power	272.24 kW	275.5 kW	275.5 kW

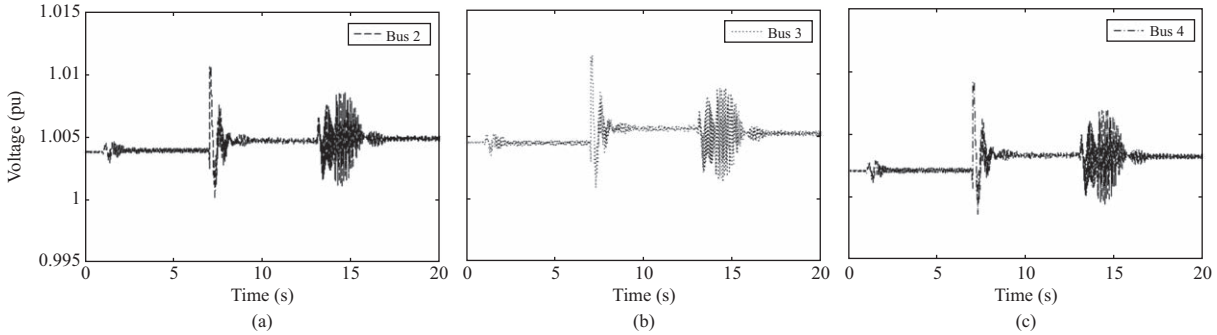

Fig. 11. Voltage responses of system buses (off-grid).

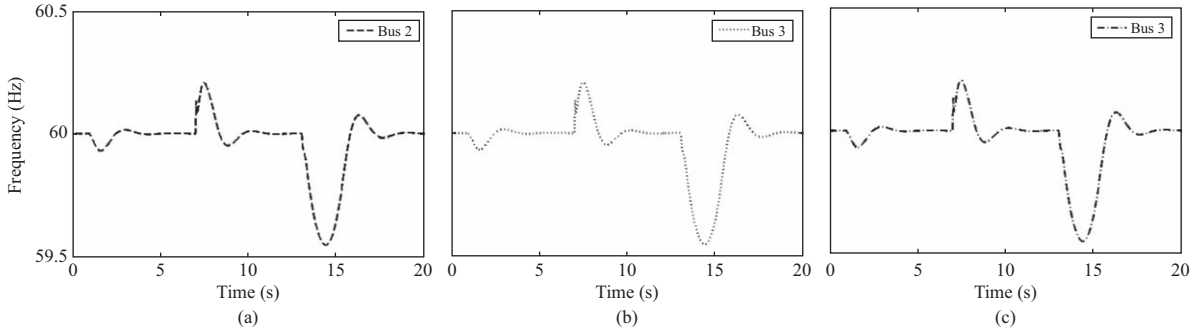

Fig. 12. Frequency responses of system buses (off-grid).

cycle use the same model to generate power. The hybrid-cycle heat quantity of evaporator and condoner are the largest, and the closed-cycle heat quantity of evaporator and condoner are the smallest. Both closed-cycle and hybrid-cycle output powers are the same. Therefore, the heat quantity of hybrid-cycle is better than the other two types of OTEC systems. From theses analyses, the hybrid-cycle and the closed-cycle perform better than the open-cycle does.

3. Power System under Off-Grid and Grid-Connected

The case study includes two system operation conditions: off-grid and grid-connected. For the first case, dynamic analysis is to be performed on the power system with OTEC system under off-grid operation. At first, the simulation work to be conducted starts with wind speed which is changed from 11 m/s to 10.8 m/s after 1 second, and the output power of wind generation decrease from 265 kW to 255 kW. And then the load decrease from 400 kW to 350 kW after 6.5 seconds. Finally, the wind speed decrease from 10.8 m/s to 10.2 m/s after 13.5 seconds, and the output power of wind generation is 206 kW. Fig. 11 and Fig. 12 show that the system voltage and frequency follow the trend of wind speed. The load demand decreases which causes the bus voltage and frequency changed. The active and reactive power responses of the system with OTEC generation under the wind

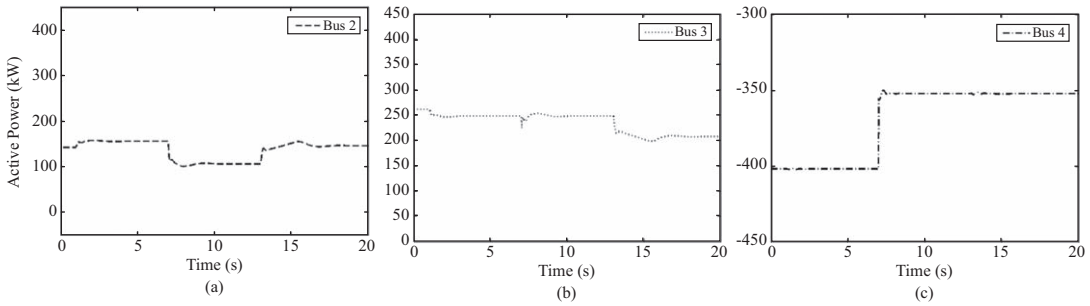

Fig. 13. Active power responses of system buses (off-grid).

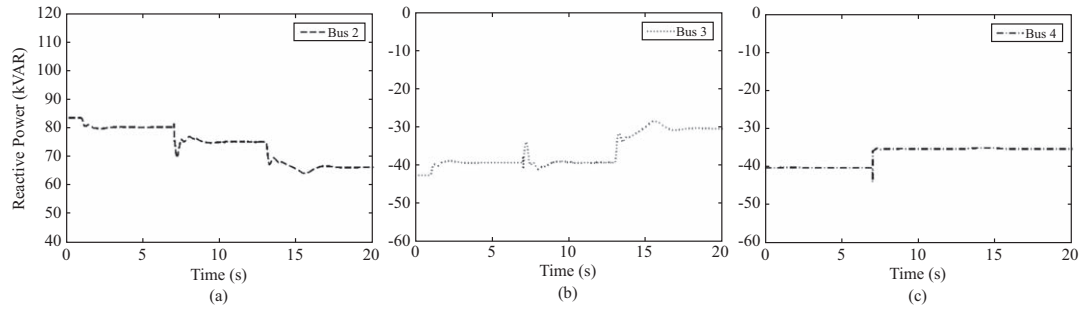

Fig. 14. Reactive power responses of system buses (off-grid).

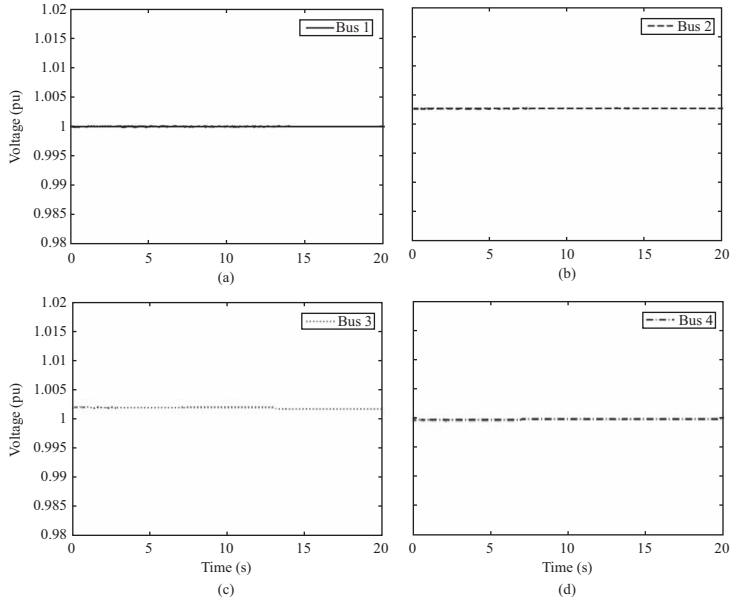

Fig. 15. Voltage responses of system buses (grid-connected).

speed decreases and load reduction are shown in Fig. 13 and Fig. 14. We can observe that the active power produced by wind generation has a drop and reactive power absorbed by wind generation decreases. The active and reactive power of OTEC generation is then adjusted to meet load demand under wind speed variation and load changes.

Now as the second case, dynamic analysis is to be performed on the power system with OTEC system under the grid-connected operation. The wind speed is set to be constant. At first, the simulation work to be conducted starts with wind speed which is changed from 11 m/s to 10.8 m/s after 1 second, and the output power of wind generation decrease from 265 kW to 255 kW. And then the load decrease from 400 kW to 350 kW after 6.5 seconds. Finally, the wind speed decrease from 10.8 m/s to 10.2 m/s after 13.5 seconds, and the output power of wind generation is 206 kW. Form Fig. 15 and Fig. 16, it has been found that the system voltage and frequency responses are less influenced under wind speed decrease because the micro-grid is operated in

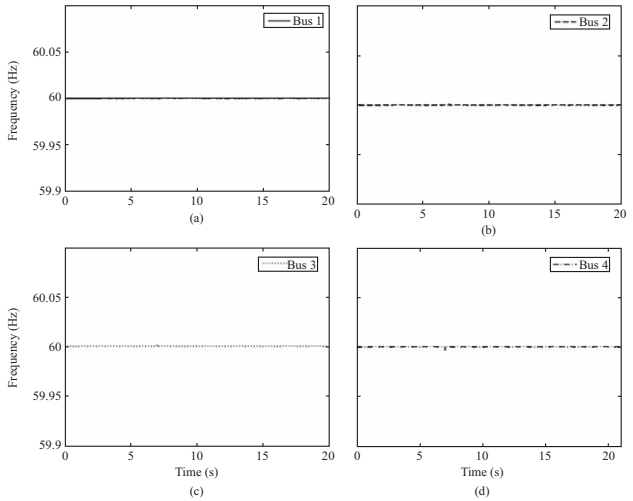

Fig. 16. Frequency responses of system buses (grid-connected).

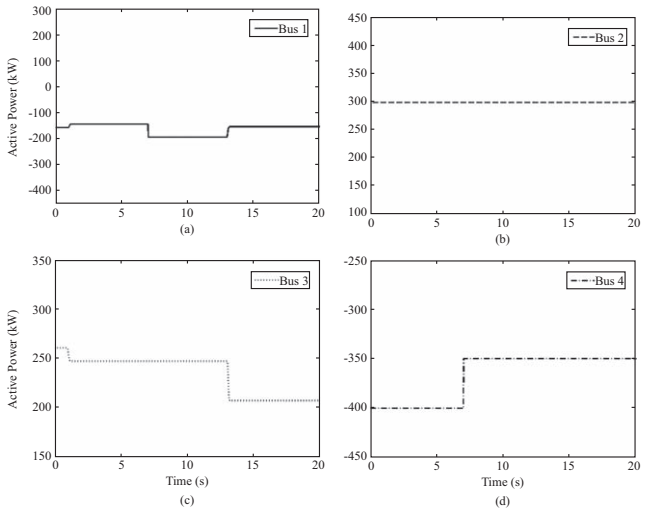

Fig. 17. Active power responses of system buses (grid-connected).

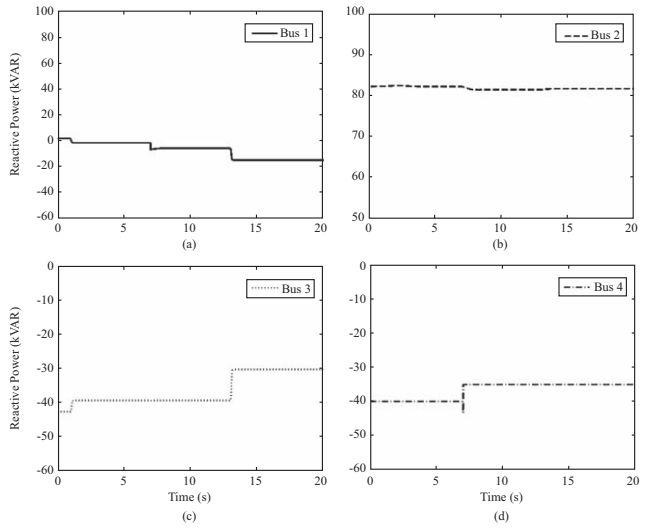

Fig. 18. Reactive power responses of system buses (grid-connected).

the grid-connected mode. The active and reactive power delivered to the load side by the power system with OTEC generation are illustrated in Fig. 17 and Fig. 18, respectively. We can observe that the output power of utility follows the trend of wind speed and load change, the active power of OTEC generation remains constant. The power system with OTEC generation can efficiently track the wind speed changes and meet the load demand.

IV. CONCLUSION

The main purpose of this paper is to analyze the dynamic responses of micro-grid with the OTEC system. Three different types of OTEC generation systems, i.e., open-cycle, closed-cycle, and hybrid-cycle are considered, under the conditions with same temperature of sea water and output of generator. The comparative analysis results show that the open-cycle generates less output power than other two types OTEC generation systems and the output power of closed-cycle is the same as hybrid-cycle. On the other hand, according to dynamic analysis of the micro-grid, when the system operates under islanding or grid-connected mode, the responses of load variation are quite different. As the system operates under the grid-connected mode, the voltage and frequency are less affected by wind speed variation and load changes; while the system operates under the islanding mode, affected voltage and frequency can be regulated by the exciter and the governor respectively and will return to a new stable state. Study results show that the OTEC system can be regarded as a steady and reliable power supply in the micro-grid.

ACKNOWLEDGEMENTS

This work was supported in part by Ministry of Science and Technology under Grant MOST 104-ET-E-019-005-ET.

REFERENCES

Ahmad, A. and A. S. Siddiqui (2014). Modeling of a wind diesel integrated system with no storage. International Journal of Emerging Technology and Advanced Engineering 4, 106-112.

Anderson, P. M. and A. A. Fouad (2002). Power System Control and Stability. John Wiley & Sons.

Avery, W. H. and C. Wu (1994). Renewable Energy from the Ocean: A Guide to OTEC. Oxford University Press.

Aydin, H. (2013). Performance analysis of a closed-cycle ocean thermal energy conversion system with solar preheating and superheating. University of Rhode Island Master's Theses.

Ghosh, T. and M. Prelas (2011). Energy Resources and Systems Volume 2: Renewable Resources. Springer Science and Business Media.

Goto, S., D. Iseri, Y. Matsuda, T. Sugi and T. Morisaki (2012). Simulation model of evaporator and separator in OTEC plant using Uehara cycle for liquid level control. Proceeding of SICE Annual Conference (SICE), 2088-2093.

Kim, A. S., H. S. Lee and S. Cha (2016). Dual-use open cycle ocean thermal energy conversion (OC-OTEC) using multiple condensers for adjustable power generation and seawater desalination. Renewable Energy 85, 344-358.

Kundur, P. (1994). Power System Stability and Control. New York, McGraw-Hill.

Lee, H.-K., J. K. Kim, B.-K. Kim and H.-J. Kim (2016). OTEC thermal dispersion in coastal waters of Tarawa, Kiribati. OCEANS 2016, 1-4.

Matsuda, Y., T. Shimada, T. Sugi, S. Goto, T. Morisaki and Y. Ikegami (2015). Controller design for liquid level control of separator in an OTEC plant with Uehara cycle considering disturbances. Proceeding of 15th International Conference on Control, Automation and Systems (ICCAS), 12-15.

Mudaliyar, S. R. and S. Mishra (2016). Dynamic stability analysis of off-shore SC-OTEC plant in a multi-machine power system. Proceeding of IEEE 6th International Conference on Power Systems (ICPS), 1-6.

Najafi, A., S. Rezaee and F. Torabi (2011). Multi-Objective optimization of ocean thermal energy conversion power plant via genetic algorithm. Proceeding of 2011 IEEE Electrical Power and Energy Conference, 41-46.

Shakil, S. R., Md. S. Hossain and N. T. Rouf (213). Proposal of possible OTEC sites in Bangladesh. Proceeding of 2013 International Conference on Electrical Information and Communication Technology (EICT), 1-5.

Urayoshi, D., Y. Matsuda, T. Sugi, S. Goto, T. Morisaki and Y. Ikegami (2014). Model construction of heat source in an OTEC pilot plant for stabilization control based on experimental data. Proceeding of 14th International Conference on Control, Automation and Systems, 116-120.

Vega, L. A. (1995). Ocean Thermal Energy Conversion, Encyclopedia of Energy Technology and the Environment. John Wiley & Sons.

Vega, L. (2002). Ocean thermal energy conversion primer. Marine Technology Society Journal 36, 25-35.

Vijayakrishna Rapaka, E., S. Rajagopan, V. Pranitha, and R. Kathambari, R. (2013). Modeling of hydrogen production through an ocean thermal energy conversion system. International Journal of Emerging Science and Engineering, 41-46.

Wang, L. and C. C. Huang (2010). Dynamic stability analysis of a grid-connected solar-concentrated ocean thermal energy conversion system. IEEE Transactions on Sustainable Energy 1, 10-18.

Yeh, R.-H., T.-Z. Su and M.-S. Yang (2004). Maximum output of an OTEC power plant. Ocean Engineering 32, 685-700.